Journal of Photochemistry and Photobiology A: Chemistry 220 (2011) 173–178

Contents lists available at ScienceDirect

Journal of Photochemistry and Photobiology A: Chemistry

journal homepage: www.elsevier.com/locate/jphotochem

The fluorescence properties of cationic rhodamine B in the gas phase

Sandeep K. Sagoo, Rebecca A. Jockusch*

Department of Chemistry, University of Toronto, Toronto, Ontario M5S 3H6, Canada

ARTICLE INFO

Article history:
Received 26 February 2011
Received in revised form 30 March 2011
Accepted 3 April 2011
Available online 12 April 2011

Keywords:
Rhodamine B
Quadrupole ion trap mass spectrometry
Gaseous ion fluorescence
Laser-induced fluorescence
Fluorescence lifetime
Xanthene dyes

ABSTRACT

Studying the photophysical properties of molecules in the gasphase can be advantageous, because it reduces the complexity of the system examined by eliminating effects due to theinteractions between the molecule of interest and other species present in the local environment, including those with the solvent itself. Here, we report on theintrinsic properties of gaseous protonated rhodamine B (RBH^+), a well-known xanthene-based dye. Protonated rhodamine B was transferred into the gas phase using electrospray ionization (ESI) and isolated in a quadrupole ion trap (QIT) mass spectrometer, which has been modified to enable laser-induced fluorescence spectroscopy of trapped ions. The gas-phase fluorescence excitation and emission spectra of RBH^+show maxima ($\lambda_{ex\,(max)}$ = 531 nm and $\lambda_{em\,(max)}$ = 542 nm, respectively)that lie at higher energy than those of RBH^+ in solution. The fluorescence lifetime of gaseous RBH^+ is 5.97 ± 0.12 ns, which is significantly longer than that of solution-phase rhodamine B. Gaseous rhodamine B is signficiantly brighter than monoethylamino rhodamines such as gaseous rhodamine 6G. Knowledge of the intrinsic photophysical properties of chromophores, such as those presented here for rhodamine B, will enable a better understanding of how the local environment of the chromophore modulates its properties.

1. Introduction

Xanthene-based dyes are one of the most extensively studied families of luminescent dyes. This class of dyes includes fluorescein, eosins, and rhodamines [1]. These dyes are used in a wide range of applications, for example, as biological stains [2], sensitizers [3], fluorescent probes [4], tracing agents [5], and laser dyes [6]. Xanthene dyes exist in a variety of neutral and ionic forms in solution. Each form usually possesses unique spectral properties, and these can be highly dependent on the local environment of the dye. Numerous studies have shown that the quantum yield, absorption and emission spectra, and fluorescence lifetimes for these dyes vary greatly depending on the solvent conditions [7–12]. Despite extensive studies of many xanthene dyes in solution, their sensitivity to solvent, compounded with concentration and temperature dependencies, have resulted in difficulties in understanding their photophysics [7–12].

A useful way to better understand the effect of solvent on these dyes is to study their intrinsic properties in the gas-phase. Using mass spectrometry the various ionic forms of a chromophore can be individually isolated and studied [13–20]. This restricts ambiguity arising from the equilibria that exist among different ionic forms of the dye and eliminates the complexity introduced by intermolecular interactions with the solvent. Comparison of gas-phase with solution-phase behavior then can be used to distinguish between intrinsic behavior and the effects of solvent. The role of individual solvent molecules can also be probed by isolating and studying gas-phase complexes and clusters containing the dye and a known number of water molecules.

Here, we report the intrinsic photophysical properties of protonated rhodamine B (RBH^+), a well-known xanthene-based dye. Rhodamine B is used as the active medium in pulsed and continuous wave lasers [21], as a staining fluorescent dye in biology [22], and as a tracer dye to track the movement of water [23]. Rhodamine B was first synthesized by Maurice Ceresole in 1887 [24] and in aqueous solution was first studied by Holmes, who determined that the absorption spectra could be explained by an equilibrium between two forms of rhodamine B [8]. In addition to the optically active protonated and zwitterionic forms, a colorless lactone form is now also known to exist. These three forms of rhodamine B are shown in Scheme 1.

The absorption and emission properties of rhodamine B are highly sensitive to the solvent environment [25,26]. Although numerous studies have been carried out to examine the properties of rhodamine B in the condensed phase, its photophysics continues to be the subject of significant debate [7,9–12,25–27,39]. Similar to other rhodamine dyes, rhodamine B has a high molar absorptivity (ε) (~106,000 $M^{-1}\,cm^{-1}$ in ethanol at 543 nm [28]). Reported fluorescence quantum yields (Φ_f) range from 0.3 to 0.66, depending on the solvent [7,9–11,29]. Fluorescence lifetimes (τ)

* Corresponding author. Tel.: +1 416 946 7198; fax: +1 416 978 8775.
E-mail address: rebecca.jockusch@utoronto.ca (R.A. Jockusch).

1010-6030/$ – see front matter © 2011 Elsevier B.V. All rights reserved.
doi:10.1016/j.jphotochem.2011.04.008

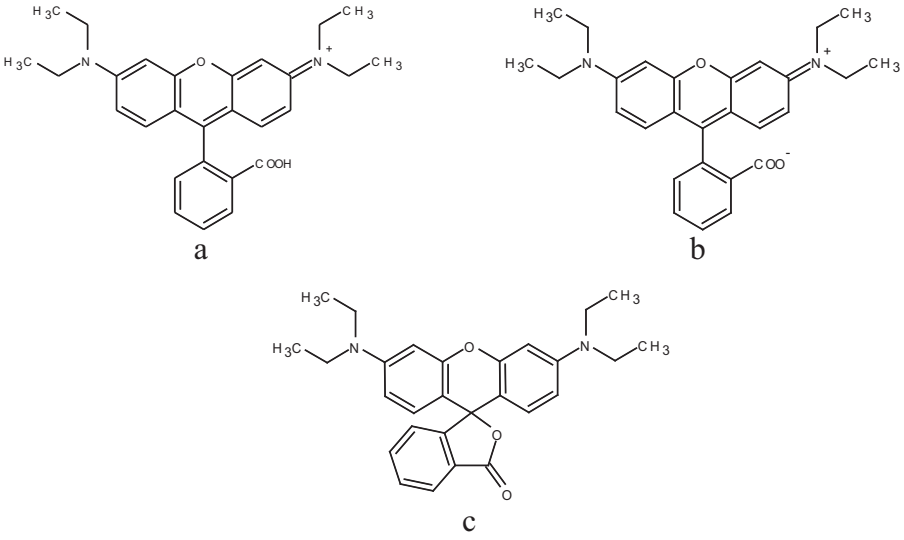

Scheme 1. Structure of rhodamine B (a) cation, RBH^+; (b) zwitterion, $RB^{\pm}$; and (c) lactone, RB.

are also strongly solvent dependent, ranging from 3.2 ns in octanol to just 1.5 ns in water [7]. The sensitivity of fluorescence lifetime and quantum yield to the solvent is attributed primarily to changes in non-radiative relaxation rates. The fundamental reason behind this variation is not well understood. One clear trend is that as the polarity of the solvent mixture increases, the quantum yield of rhodamine B decreases [9,11,30]. Some studies have also identified solvent viscosity as an important contributing factor in rhodamine B's solvent sensitivity; in a high viscosity solvent, motion of the flexible diethylamino groups on the xanthene ring is restricted, which could lower non-radiative decay rates [6,7,9,30]. However, other studies have discounted this suggestion, finding no direct dependence of the non-radiative decay rates on solvent viscosity [10,11,31]. Specific mode coupling between vibrations of rhodamine B and those of interacting solvent molecules have also been invoked to explain the large variation in non-radiative decay rate [9,32]. The identity of the solvent also affects the position of the absorption and emission maxima for rhodamine B. For cationic rhodamine B in methanol, these values are 552 nm and 577 nm, respectively, whereas in water, there is a small red-shift of the respective maxima to 557 nm and 580 nm [11,25]. This red-shift has been attributed to a greater stabilization of the highly polarizable excited state with respect to the ground state due to more favorable interactions between the dye and polar solvents, which leads to a decrease in the $S_0 \rightarrow S_1$ energy level gap [17,19,33].

Reports on the properties of gas-phase rhodamine B are sparse. The absorption and emission maximafor the *neutral* form of rhodamine B, transferred into the gas phase by heating, were shown to occur at significantly shorter wavelengths (435 nm and 525 nm, respectively) compared with the corresponding bands in ethanol (540 nm and 575 nm, respectively) [33]. Very recently, Zenobi and coworkers have studied the *neutral* form of a different rhodamine, rhodamine 19 (R19, also known as rhodamine 575), by forming complexes with metal cations ($R19 + M^+$), in the gas-phase [34]. Photodissociation action spectra of the complexed *neutral* form of R19 also indicate a blue shift in absorption upon transfer from solution to the gas phase. This blue shift in fluorescence excitation and/or emission maxima upon transfer from solution to the gas phase has been reported for several other ionic xanthene dyes [13–16,26,34,35], including a well-known series of protonated monoethylamino-rhodamine dyes (rhodamine 575, 590 and 6G) [15].

In this work, we investigate the intrinsic properties of gaseous RBH^+ using a trapping mass spectrometer which has been modified to enable laser excitation and fluorescence detection of the trapped ions. A major benefit of using a trapping mass spectrometer for these studies is the ability to mass select and store the ion of interest, eliminating the need for solution phase purification and uncertainty about the identity of the fluorescing species. Fluorescence emission and excitation spectra, as well as the fluorescence lifetime of gaseous cationic rhodamine B (RBH^+) are reported and compared with pre-existing theoretical calculated values [36] as well as literature solution-phase data.

2. Experimental methods

Rhodamine B (Scheme 1) was supplied by Sigma–Aldrich Canada Ltd. (Oakville, ON) and used without further purification. Solutions for electrospray ionization (ESI) were prepared by dissolving the dye in 50:50 methanol/water solutions to a concentration of 0.1 μM. Mass spectra were recorded using a modified commercial quadrupole ion trap (QIT) mass spectrometer (Bruker Esquire 3000+, BrukerDaltonik, Germany) equipped with an ESI source[16]. The solution was infused at a flow rate of 2.5 μL/min with a concurrent flow of N_2 nebulization gas (11–28 psi) through the electrospray emitter. Counter-current drying gas (also N_2) was fixed at 3.5 L/min at a temperature of 300 °C. In the Bruker ESI source, the ESI emitter is held at ground while the entrance of the capillary inlet to the mass spectrometer was adjusted to –(3000–3200) V. The ion accumulation timewas set to maintain an ion charge control (ICC) value of $\sim 1 \times 10^6$ for all fluorescence experiments. This ICC value corresponds to an estimated ion number of $\sim 5 \times 10^4$ [16]. Ions are held in the QIT by an electrodynamic trapping field at trapping parameter q_z of 0.59, and are subject to collisions with $\sim 3 \times 10^{-3}$ mbar of room temperature helium bath gas, which serves to focus the ion cloud to the center of the trapping electrodes and to remove excess internal energy from the trapped molecular ions. At this pressure, the collision rate between the trapped molecular ions and the helium bath gas is $\sim 10^5\ s^{-1}$.

RBH^+ ions generated by ESI were mass-selected and stored in the QIT where they were irradiated with the frequency-doubled output of a mode-locked Titanium:Sapphire laser (Tsunami, Spectra-Physics, Mountain View, CA pumped by a 10 W Millenia Pro; 80 MHz repetition rate, ~130 fs pulse duration). Upon second har-

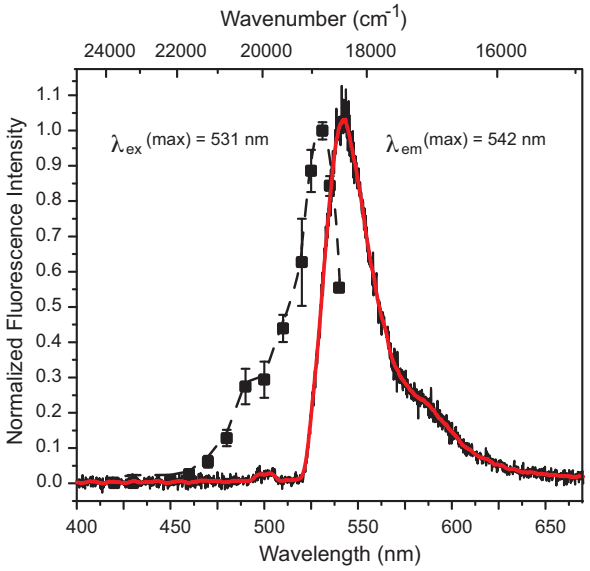

Fig. 1. Fluorescence excitation (squares) and emission (solid line) spectra for cationic rhodamine B (RBH^+) in the gas phase.

monic generation, visible light in the range of 350–540 nm can be generated from this laser source. The laser beam enters and exits through two holes in the ring electrode of the QIT, thus intersecting the cloud of trapped, mass-selected ions. Fluorescence is collected through a third hole in the ring electrode which is orthogonal to the path of the laser beam. The collected fluorescence light is directed through an appropriate filter (Chroma Technology Corp., Rockingham, VT) and focused on the slit of a spectrograph (Shamrock303i, Andor Technologies, Belfast, Ireland) which disperses the light onto an electron-multiplied charge-coupled device detector (Newton EM-CCD, Andor Technologies, Belfast, Ireland). The EM-CCD was cooled and operated with electron multiplying features activated. More detailed information about this experimental set-up can be found elsewhere [16,37].

Fluorescence spectra were measured by irradiation of isolated ion populations with 2 mW laser power for 2 s. Following the irradiation period, the ions were scanned out of the QIT and a mass spectrum was recorded. The laser power and irradiation time used for fluorescence measurements were selected to ensure that fragmentation of the RBH^+ precursor ion, which would be visible in the recorded mass spectra, did not occur. (A photodissociation mass spectrum, recorded with higher laser power and longer irradiation time, is shown in Fig. S.1-a.) We note also that collisions with the helium bath gas help suppress ion heating and fragmentation upon irradiation [15,16]. Emission spectra recorded from 20 different ion populations were averaged at each excitation wavelength. The emission spectra were background-subtracted using spectra recorded under identical conditions but without any ions in the trap. The fluorescence emission spectrum of RBH^+ ions shown was measured using 500 nm laser excitation with a 515 nm long pass filter. The spectrum was processed with a 1st-order, 25 point, Savitzky–Golay digital filter and is the thick solid trace shown in Fig. 1. The excitation spectrum was produced by measuring the fluorescence intensity upon irradiation at a series of excitation wavelengths between 420 and 532 nm, stepping in 5–10 nm intervals. A band pass (546–610 nm) filter was used in the detection path and the fluorescence intensity at each excitation wavelength was taken as the integrated emission intensity between 550 and 610 nm. The excitation spectrum shown is the average of four separate measurements. The error shown corresponds to ± one standard deviation of the four replicate measurements.

A few modifications to the instrumentation described enabled fluorescence lifetime measurements. A pulse picker was used in the excitation beam path to pick one out of three pulses in a train of pulses, thus increasing the time between laser pulses from 12.5 ns to 37.5 ns in order to ensure sufficient time for fluorescence decay between laser pulses. For detection, the fluorescence emission from the trapped ions was sent through a 515 nm long pass filter and then directed towards an infinity corrected objective (RMS10X, Thorlabs, Newton, NJ), which focuses the light onto a Single-Photon Avalanche Diode (SPAD – PDM Series, Micro Photon Devices, QC). Concurrently, the laser beam exiting the QIT was sent onto a fast photodiode (Thorlabs, Newton, NJ) and the signals from both the SPAD and photodiode detectors were sent to a Time-Correlated Single-Photon Counting (TCSPC) card, model TimeHarp 200 (PicoQuant GmbH, Berlin, Germany) to record the fluorescence decays. Fluorescence decays for RBH^+ were obtained by irradiating multiple populations of trapped, mass-selected ions, each with 4 mW at 510 nm for 5 s irradiation times, to a total of 1200 s. No photodissociation of the precursor ion was observed in the subsequently recorded mass spectra. The reported error in fluorescence lifetime indicates one standard deviation from three replicate measurements.

3. Results and discussion

3.1. Emission and excitation spectroscopy

3.1.1. Gas-phase fluorescence spectra

The fluorescence excitation and emission spectra for gaseous cationic rhodamine B are shown in Fig. 1. The maximum excitation ($\lambda_{ex\,(max)}$) and emission ($\lambda_{em\,(max)}$) wavelengths are 531 nm and 542 nm, respectively. The Stokes shift, the energy difference between the emission and excitation maxima, is 380 cm^{-1}. The emission and excitation spectra have a distinct mirror-image like quality. There is a shoulder, presumably due to a strong vibronic transition between S_0 and S_1, ~1400 cm^{-1} below the emission maximum and this is mirrored by a shoulder present at ~1570 cm^{-1} above the excitation maximum. The small Stokes shift and the mirror-image quality of the fluorescence excitation and emission spectra indicate that the geometry change between the ground and electronically excited states of rhodamine B in the gas-phase is small.

Unexpectedly, we found that gaseous RBH^+ is approximately two-fold brighter than gaseous protonated rhodamine 575 (for which $\Phi_f = 0.82$ and $\varepsilon = 82{,}000\ M^{-1}\ cm^{-1}$ in ethanol [38]) (see Fig. S.2) which means that it is brighter than the well-known rhodamine 6G by ~50% in the gas phase [15]. The difference in brightness was the same upon excitation near each dye's $\lambda_{ex\,(max)}$ and upon excitation of the vibronic shoulder (see supplementary information for more details). While part of this difference in brightness may be due to differing absorptivities, the magnitude of the difference ($R575H^+$:$R6GH^+$:RBH^+ ~ 1.0:1.3:2.0) suggests that the fluorescence quantum yield of gaseous RBH^+ may be higher than that of gaseous $R575H^+$ and $R6GH^+$. This would be the reverse of their relative quantum yields in solution, in which protonated rhodamine B has a significantly lower quantum yield (0.3–0.66) [9–11,29] than protonated rhodamine 575 (0.8) or rhodamine 6G (0.95). If this is the case, the implication is that interactions between RBH^+ and solvent molecules provide significantly better deactivation pathways than those between the solvent and monoethylamino rhodamines such as R575 and R6G.

3.1.2. Comparison of gas-phase and solution-phase fluorescence spectra

The most striking difference between the experimental gas-phase data and literature solution-phase data is that the solution-phase fluorescence absorption and emission maxima are red-shifted compared to the gas-phase fluorescence excitation and emission maxima (by $-720\,cm^{-1}$ and $-1120\,cm^{-1}$, respectively in methanol solutions [11] and $-880\,cm^{-1}$ and $-1210\,cm^{-1}$, respectively in aqueous solutions [25]). This presumably reflects a larger $S_0 \rightarrow S_1$ energy gap in the gas-phase than in methanol or water solutions, consistent with a more highly polarizable excited state being better stabilized than the ground state due to solvent interactions [17,19,33]. Similar red shifts in the absorption of rhodamine cations upon solvation have also been reported in previous experimental and computational studies [14–16,26,34], and by Pappalardo and Ahmed who studied vapour phase neutral RB [33].

Setiawan et al. have examined solvent effects on the spectroscopy of RBH^+ computationally using time-dependent density functional theory (TD-DFT) and several different levels of theory [36]. Solvent effects were included via a conductor-like polarizable continuum model. Calculations at the BLYP/6-311G* level of theory found the $S_0 \rightarrow S_1$ transition to lie at 512 nm in the gas-phase and at 528 nm in water. The predicted solvent shift ($-613\,cm^{-1}$) is in the same direction as seen by experiment, but it is somewhat smaller than what is actually observed ($-880\,cm^{-1}$). While the BLYP density functional was identified as being the most accurate in that report since it gave an excitation maximum in water (528 nm) that is closest to the literature value (557 nm) [25], it is interesting to note the other methods used (B3LYP, BH&HLYP, and HF) predicted solvent shifts ($-863\,cm^{-1}$, $-939\,cm^{-1}$, and $-891\,cm^{-1}$, respectively) that were closer to the experimental solvent shift. However, these other functional/basis set combinations gave excitation maxima that were much higher in energy (463–361 nm gas phase, 373–482 nm aqueous) than experimental values of 531 nm (gas phase) and 557 nm (aqueous).

The observed fluorescence Stokes shift for gaseous RBH^+ ($380\,cm^{-1}$) is approximately half that of RBH^+ solvated in methanol ($785\,cm^{-1}$), consistent with a smaller change in molecular geometry from $S_0 \rightarrow S_1$ in the gas phase than in solution. This is not surprising, given that solvent relaxation is expected to occur around the excited RBH^+, which would result in further geometrical changes in the excited solvated dye.

3.2. Fluorescence lifetime

The measured fluorescence decay for gas-phase RBH^+, with the corresponding fit by an exponential decay convoluted with a Gaussian instrument response function, is shown in Fig. 2. The fluorescence decay of RBH^+ in the gas phase is well fit by a single exponential with a lifetime of $\tau_{gas} = 5.97 \pm 0.12$ ns. This is significantly longer than that of the dye in octanol (3.2 ns) or water (1.5 ns) [7]. Other cationic rhodamine dyes, as well as other fluorophores such as fluoranthene and BODIPY-TMR, have similarly been found to have longer lifetimes in the gas-phase than in solution [40–45]. We note that the gas-phase fluorescence lifetime reported here is not affected by the presence of helium bath gas within the trap because the measured lifetime (~6 ns) is significantly shorter than the average time between collisions, which is approximately one collision every 10 μs at the pressure of helium used.

The increase in the fluorescence lifetime for rhodamine B in vacuum must correspond to a decrease in the radiative (k_r) and/or non-radiative (k_{nr}) rate constants (Eq. (1)).

$$\tau = \frac{1}{k_r + \Sigma k_{nr}} \quad (1)$$

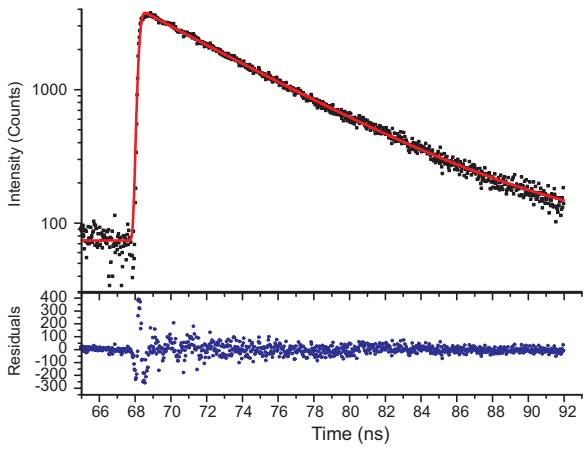

Fig. 2. Fluorescence decay for gas-phase RBH^+. Fit to the data is shown as a solid line.

In solution, k_r for RBH^+ has been calculated to vary little ($1.7–2.3 \times 10^8\,s^{-1}$), regardless of the type of solvent (i.e. in water or a series of alcohols) [7,9,11,30]. On the other hand, the non-radiative rate (attributed primarily to internal conversion) is much more sensitive to the solvent, ranging from 1.7 to $4.6 \times 10^8\,s^{-1}$ in the same solvent series [9,11,30].

The increase in the fluorescence lifetime when going from the condensed phase to vacuum is in part due to a decrease in k_r because of the lower index of refraction (n) in vacuum. This effect can be estimated using a simple model (Eq. (2)) which links the gas- and solution-phase radiative rates by [46,47]:

$$k_{r(soln)} \approx \frac{n_{soln}^2}{n_{gas}^2} \frac{\varepsilon_{soln}(\lambda)}{\varepsilon_{gas}(\lambda)} k_{r(gas)} \quad (2)$$

where ε is the molar absorptivity in solution or in vacuum at a particular wavelength. Unfortunately, ε_{gas} cannot be measured in our present experimental set-up because of the low ion density and short optical path length. We note however that in principle this can be done; Kondow and coworkers recently successfully coupled cavity ring-down spectroscopywith a quadrupole ion trap to directly determine the optical absorption cross section of metal ions and metal ion clusters [48,49].

Assuming that the difference in absorptivities between a given molecule in solution and in the gas phase is negligible, Eq. (2) can be simplified to give Eq. (3):

$$k_{r(gas)} \sim k_{r(soln)} \frac{n_{gas}^2}{n_{soln}^2} \quad (3)$$

This simplifying assumption seems reasonable given that the estimated difference in molar absorptivities of RBH^+ in solution and in vacuum is less than 2% according to both the Lorentz virtual cavity model and the empty spherical cavity models [46]. The refractive index in solution is higher ($n_{methanol} = 1.329$) [50] than that of vacuum ($n_{gas} = 1$), so this simple model suggests that the radiative rate decay constant in the gas-phase should be roughly half ($\sim 1.3 \times 10^8\,s^{-1}$) that in solution phase ($\sim 2.3 \times 10^8\,s^{-1}$ in methanol) [9], which would contribute to the longer fluorescence lifetime of RBH^+ in the gas phase.

A decrease in non-radiative decay rates can also contribute to the longer fluorescence lifetime of gaseous RBH^+ (Eq. (1)). The non-radiative rates in vacuum can be estimated from Eq. (4), which results from rearrangement of Eq. (1) followed by substitution by Eq. (3). Using literature values for $k_{r(soln)}$ and n_{soln} [9,11,30], the assumption made above that absorptivities do not change between the gas and solution phases and the experimental gas-

phase lifetime of $\tau_{gas} = 5.97$ ns, we arrive at a range of values for $k_{nr(gas)}$ of $\sim 0.4–0.7 \times 10^8\ s^{-1}$. These values are 4–6 times lower than the reported solution-phase radiative rates ($1.7–4.6 \times 10^8\ s^{-1}$) [9,11,30] which further explains the longer fluorescence lifetime in vacuum. A substantially lower non-radiative rate for gaseous RBH^+ is also consistent with our speculation that the relative brightness of RBH^+ results from a fluorescence quantum yield that is significantly higher in the gas phase than in solution. This also supports the idea that coupling between the solvent and the chromophore provides an important non-radiative decay pathway [9,32].

$$\Sigma k_{nr(gas)} \sim \frac{1}{\tau_{gas}} - \frac{k_{r(soln)}}{n^2_{soln}} \quad (4)$$

4. Conclusions

The intrinsic (gas-phase) properties of cationic rhodamine B were determined using quadrupole ion trap mass spectrometry coupled with laser-induced fluorescence spectroscopy. The measured excitation and emission maxima for RBH^+ lie at higher energy in the gas phase than in the solution phase and the fluorescence lifetime for the cationic form of rhodamine B in the gas phase is much longer than in solution phase.

This study is part of our laboratory's effort to determine the intrinsic photophysical properties of various ionic dyes in a controlled gas-phase environment [15,16,35,40]. We are building up a library of the intrinsic properties of ionic fluorophores. This data will provide a baseline from which to better understand solvent effects. In addition to comparisons with bulk solvation, our instrumentation allows isolation of specific complexes of the fluorophores and a known number of solvent molecules. The optical properties of the fluorophores in well-defined microenvironments can thus be studied. Another application of this fundamental research is to enable selection and characterization of appropriate donor and acceptor fluorophore pairs to carry out gas-phase fluorescence resonance energy transfer (FRET) experiments [51–53]. These show promise as a novel way to determine the conformation of larger molecules, such as proteins, in isolation and thus investigate the role of the solvent in protein folding; however, they are hampered currently by the relative lack of knowledge about the properties of gaseous chromophores.

Acknowledgements

Support for this project was provided by the Canada Foundation for Innovation (CFI), the Ontario Research Fund, and Early Research Award from the Province of Ontario, the Natural Sciences and Engineering Research Council (NSERC) of Canada and the Canada Research Chairs Program.

Appendix A. Supplementary data

Supplementary data associated with this article can be found, in the online version, at doi:10.1016/j.jphotochem.2011.04.008.

References

[1] R.D. Lillie, Conn's Biological Stains, Williams & Wilkins, Baltimore, 1991.
[2] A.J. Emery, F.K. Hazen, E. Stotz, Spectrophotometric characteristics and assay of biological stains III. The xanthenes, Biotech. Histochem. 25 (4) (1950) 201–208.
[3] A.W.H. Mau, O. Johansen, W.H.F. Sasse, Xanthene dyes as sensitizers for the photoreduction of water, Photochem. Photobiol. 41 (5) (1985) 503–509.
[4] M. Beija, C.A.M. Afonso, J.M.G. Martinho, Synthesis and applications of rhodamine derivatives as fluorescent probes, Chem. Soc. Rev. 38 (2009) 2410–2433.
[5] J.M. Jamison, K. Krabill, A. Hatwalkar, E. Jamison, C. Tsai, Potentiation of the antiviral activity of poly r(A-U) by xanthene dyes, Cell Biol. Int. Rep. 14 (12) (1990) 1075–1084.
[6] K.H. Drexhage, Structure and properties of laser dyes, in: F.P. Schäfer (Ed.), Topics in Applied Physics, vol. 1, Dye Lasers, Springer-Verlag, Berlin, 1990.
[7] D. Magde, G.E. Rojas, P.G. Seybold, Solvent dependence of the fluorescence lifetimes of xanthene dyes, Photochem. Photobiol. 70 (5) (1999) 737–744.
[8] W.C. Holmes, The influence of variation in concentration on the absorption spectra of dye solutions, Ind. Eng. Chem. 16 (1) (1924) 35–40.
[9] M.J. Snare, F.E. Treloar, K.P. Ghiggino, P.J. Thistlethwaite, The photophysics of rhodamine B, J. Photochem. 18 (4) (1982) 335–346.
[10] T.L. Arbeloa, F.L. Arbeloa, P.H. Bartolome, I.L. Arbeloa, On the mechanism of radiationless deactivation of rhodamines, Chem. Phys. 160 (1) (1992) 123–130.
[11] T.L. Chang, H.C. Cheung, Solvent effects on the photoisomerization rates of the zwitterionic and the cationic forms of rhodamine B in protic solvents, J. Phys. Chem. 96 (12) (1992) 4874–4878.
[12] P.J. Sadkowski, G.R. Fleming, Photophysics of the acid and base forms of rhodamine B, Chem. Phys. Lett. 57 (4) (1978) 526–529.
[13] K.C. Wright, M.W. Blades, Fluorescence emission spectroscopy of trapped molecular ions, in: Proc. 51st ASMS Conf. Mass Spectrom, Allied Topics, Montreal, Canada, 2003.
[14] N.A. Sassin, S.C. Everhart, J.I. Cline, K.M. Ervin, Photodissociation and collisional cooling of rhodamine 575 cations in a quadrupole ion trap, J. Chem. Phys. 128 (23) (2008) 234305–234317.
[15] M.W. Forbes, R.A. Jockusch, Gas-phase fluorescence excitation and emission spectroscopy of three xanthene dyes (rhodamine 575, rhodamine 590 and rhodamine 6G) in a quadrupole ion trap mass spectrometer, J. Am. Soc. Mass Spectrom. 22 (1) (2011) 93–119.
[16] Q. Bian, M.W. Forbes, F.O. Talbot, R.A. Jockusch, Gas-phase fluorescence excitation and emission spectroscopy of mass-selected trapped molecular ions, Phys. Chem. Chem. Phys. 12 (11) (2010) 2590–2598.
[17] M. Dashtiev, V. Azov, V. Frankevich, L. Scharfenberg, R. Zenobi, Clear evidence of fluorescence resonance energy transfer in gas-phase ions, J. Am. Soc. Mass Spectrom. 16 (9) (2005) 1481–1487.
[18] Y. Wang, C.L. Hendrickson, A.G. Marshall, Direct optical spectroscopy of gas-phase molecular ions trapped and mass-selected by ion cyclotron resonance: laser-induced fluorescence excitation spectrum of hexafluorobenzene ($C_6F_6^+$), Chem. Phys. Lett. 334 (2001) 69–75.
[19] J.T. Khoury, S. Rodriguez-Cruz, J.H. Parks, Pulsed fluorescence measurements of trapped molecular ions with zero background detection, J. Am. Soc. Mass Spectrom. 13 (6) (2002) 696–708.
[20] V. Frankevich, X. Guan, M. Dashtiev, R. Zenobi, Laser-induced fluorescence of trapped gas-phase molecular ions generated by internal source matrix-assisted laser desorption/ionization in a Fourier transform ion cyclotron resonance mass spectrometer, Eur. J. Mass Spectrom. 11 (5) (2005) 475–482.
[21] T. Erwin, Ullmann's Encyclopedia of Industrial Chemistry, Wiley-VCH Verlag GmbH & Co, Weinheim, 2000.
[22] W.B. Shelley, Fluorescent staining of elastic tissue with rhodamine B and related xanthene dyes, Histochem. Cell Biol. 20 (3) (1969) 244–249.
[23] M. Flury, N.N. Wai, Dyes as tracers for vadose zone hydrology, Rev. Geophys. 41 (2003) 1–37.
[24] M. Ceresole, D.R. Patent 44002, (1887).
[25] I.L. Arbeloa, K.K. Rohatgi-Mukherjee, Solvent effect on photophysics of the molecular forms of rhodamine B. Solvation models and spectroscopic parameters, Chem. Phys. Lett. 128 (1986) 474–479.
[26] P.C. Jha, Y. Wang, H. Agren, Two-photon absorption cross-sections of reference dyes: a critical examination, Chem. Phys. Chem. 9 (2008) 111–116.
[27] I.L. Arbeloa, P.R. Ojeda, Molecular forms of rhodamine B, Chem. Phys. Lett. 79 (2) (1981) 347–350.
[28] H. Du, R.A. Fuh, J. Li, A. Corkan, J.S. Lindsey, PhotochemCAD†: a computer-aided design and research tool in photochemistry, Photochem. Photobiol. 68 (2) (1998) 141–142.
[29] R.F. Kubin, A.N. Fletcher, Fluorescence quantum yields of some rhodamine dyes, J. Lumin. 27 (4) (1982) 455–462.
[30] K.G. Casey, E.L. Quitevis, Effect of solvent polarity on nonradiative processes in xanthene dyes: rhodamine B in normal alcohols, J. Phys. Chem. 92 (23) (1988) 6590–6594.
[31] H. Alobaidi, F. Alberkdar, Z. Hafidh, S. Alalkway, in: K.L. Kompa, S.D. Smith (Eds.), Laser Induced Processes in Molecules, Springer, Berlin, 1979, pp. 108–110.
[32] J.A.B. Ferreira, S.M.B. Costa, Activationlessnonradiative decay in rhodamines: role of NH and lower frequency vibrations in solvent kinetic isotope effects, Chem. Phys. 321 (2006) 197–208.
[33] R. Pappalardo, S. Ahmed, Emission from dyes in the vapor phase and the possibility of vapor phase dye lasers, J. Chem. Phys. 56 (10) (1972) 5135–5144.
[34] K. Chingin, R.M. Balabin, V. Frankevich, H. Chen, K. Barylyuk, R. Nieckarz, A. Fedorov, R. Zenobi, Rhodamines in the gas phase: cations, neutrals, anions, and adducts with metal cations, Phys. Chem. Chem. Phys. 37 (12) (2010) 11710–11714.
[35] P.D. McQueen, S. Sagoo, H. Yao, R.A. Jockusch, On the intrinsic photophysics of fluorescein, Angew. Chem. Int. Ed. 49 (2010) 9193–9196.
[36] D. Setiawan, A. Kazaryan, M.A. Martoprawiro, M. Filatov, A first principles study of fluorescence quenching in rhodamine B dimers: how can quenching occur in dimeric species? Phys. Chem. Chem. Phys. 37 (12) (2010) 11238–11244.

[37] M.W. Forbes, F.O. Talbot, R.A. Jockusch, in: R.E. March, J.F. Todd (Eds.), Practical Aspects of Trapped Ion Mass Spectrometry, vol. 5, Applications of Ion Trapping Devices, CRC Press, Boca Raton, 2009.
[38] F.L. Arbeloa, T.L. Arbeloa, E.G. Lage, I.L. Arbeloa, F.C. Deschryver, Photophysical properties of rhodamines with monoethylamino groups R19 and R6G in water—ethanol mixtures, Photochem. Photobiol. A-Chem. 56 (1991) 313–321.
[39] F.L. Arbeloa, T.L. Arbeloa, M.J.T. Estevez, I.L. Arbeloa, Photophysics of rhodamines: molecular structure and solvent effects, J. Phys. Chem. 95 (6) (1991) 2203–2208.
[40] A. Nagy, F.O. Talbot, M.F. Czar, R.A. Jockusch, in preparation.
[41] K. Mattias, S. Detlef, N. Christian, W. Lars, M.K. Manfred, Laser-induced fluorescence of rhodamine 6G cations in the gas phase: a lower bound to the lifetime of the first triplet state, J. Phys. Chem. A 114 (17) (2010) 5509–5514.
[42] J. Friedrich, J. Fu, C.L. Hendrickson, A.G. Marshall, Y. Wang, Time resolved laser-induced fluorescence of electrosprayed ions confined in a linear quadrupole trap, Rev. Sci. Instrum. 75 (11) (2004) 4511–4516.
[43] A.T. Iavarone, J. Meinen, S. Schulze, J.H. Parks, Fluorescence probe of polypeptide conformational dynamics in gas phase and in solution, Int. J. Mass Spectrom. 253 (3) (2006) 172–180.
[44] Z. Cao, K. Balasubramanian, M.G. Calvert, H. Nitsche, Solvation effects on isomeric preferences of curium(III) complexes with multidentate phosphonopropionic acid ligands: CmH_2PPA^{2+} and $CmHPPA^{+}$ complexes, Inorg. Chem. 48 (20) (2009) 9700–9714.
[45] L.J. Jandris, R.K. Force, S.C. Yang, Fluorescence lifetime and oxygen quenching rate of gas-phase fluoranthene excited at 337.1 nm, Appl. Spectrosc. 39 (2) (1985) 266–268.
[46] D. Toptygin, Effects of the solvent refractive index and its dispersion on the radiative decay rate and extinction coefficient of a fluorescent solute, J. Fluoresc. 13 (3) (2003) 201–219.
[47] J.R. Lakowicz, Principles of Fluorescence Spectroscopy, third ed., Springer, New York, 2006.
[48] A. Terasaki, T. Majima, C. Kasai, T. Kondow, Photon-trap spectroscopy of size-selected free cluster ions: "direct" measurement of optical absorption of Ag_9^{+}, Eur. Phys. J.D. 52 (2009) 43–46.
[49] A. Terasaki, T. Majima, T. Kondow, Photon-trap spectroscopy of mass-selected ions in an ion trap: optical absorption and magneto-optical effects, J. Chem. Phys. 127 (2007) 2311011–2311014.
[50] E. Hecht, Optics: International Edition, Pearson Higher Education, New Jersey, 2002.
[51] F.O. Talbot, A. Rullo, H. Yao, R.A. Jockusch, Fluorescence resonance energy transfer (FRET) in gaseous, mass-selected polyprolinepeptides, J. Am. Chem. Soc. 132 (2010) 16156–16164.
[52] A. Danell, J.H. Parks, FRET measurements of trapped oligonucleotide duplexes, Int. J. Mass Spectrom. 229 (2003) 35–45.
[53] M. Dashtiev, V. Azov, V. Frankevich, L. Scharfenberg, R. Zenobi, Clear evidence of fluorescence resonance energy transfer in gas-phase ions, J. Am. Soc. Mass Spectrom. 16 (2005) 1481–1487.